Josephson Effect in Nb/Au/YBCO Heterojunctions

Gennady A. Ovsyannikov, *Member, IEEE*, Philippe V. Komissinski, Evgeni Il'ichev, Yuli V. Kislinski, and Zdravko G. Ivanov

***Abstract*—c-axis oriented and 11° tilted $YBa_2Cu_3O_x$ (YBCO) thin films were deposited on (110) $NdGaO_3$ and (7 10 2) $NdGaO_3$ substrates correspondingly. Nb/Au/YBCO heterojunctions were fabricated using photolithography and ion beam milling. I–V curves of the heterojunctions based on tilted YBCO films showed zero bias anomaly conductance peak and large excess current. We observed the second harmonic $(\propto \sin 2\varphi)$ of superconducting current in Nb/Au/YBCO heterojunctions in c-axis oriented YBCO films, although sinusoidal superconducting current-phase relation has been measured for heterojunctions in tilted ones. The obtained results are explained by $d \pm s$ symmetry of YBCO superconducting order parameter.**

***Index Terms*—c-axis oriented YBCO films, heterojunctions, Josephson effect, superconducting current-phase relation.**

I. Introduction

The presence of the superconducting order parameter with dominant d_{x-y}^{2-2} (d)-wave symmetry is now well established in the most of the cuprate superconductors (D) (see review [1]). In orthorhombic material, such as $YBa_2Cu_3O_x$ (YBCO), a finite s-wave component is admixed and does change sign across the twin boundary [2], [3]. In S/D-heterojunctions (/denotes a tunnel barrier) even in (001) and (110) orientations of D (S is a superconductor with a pure s-wave symmetry of the order parameter, for example Pb or Nb) this results in presence of both first $(\propto \sin\varphi)$ and second $(\propto \sin 2\varphi)$ harmonics in fthe superconducting current-phase relation (CPR) [4]. In this paper we report our results on two types of Nb/Au/YBCO heterojunctions (HJ): HJ in (001)-oriented YBCO films, where current flows mainly along c-axis of YBCO films (c-HJ); and HJ in (1 1 20)-oriented (tilted) YBCO films (t-HJ), where c-axis of YBCO film is turned through the angle of 11°. In the latter HJ current flows in the ab-plane of YBCO due to a lower Au/YBCO interface resistance in the ab-plane than in c-axis of YBCO [5].

II. Experiment

150 nm thick epitaxial YBCO films were obtained using pulsed laser deposition at 760–780°C in 0.6 mbar of O_2. We used (100) $SrTiO_3$ or (110) $NdGaO_3$ and (7 10 2) $NdGaO_3$ substrates to grow (001)- and (1 1 20)-oriented YBCO films correspondingly (see Fig. 1). The deposition conditions of YBCO films on $SrTiO_3$ and $NdGaO_3$ substrates were slightly different. The resulting YBCO films have the critical temperature of the superconducting transition (T_c) ranging from 85 to 89 K, determined by the magnetic inductive measurements. The in-plane critical current densities (J_c) for (001) and (1 1 20) YBCO films are higher than 5×10^6 A/cm^2 and 5×10^4 A/cm^2 at 77 K correspondingly. X-ray diffraction analysis indicated the uni-domain structure of the obtained YBCO films for both investigated film orientations.[1]

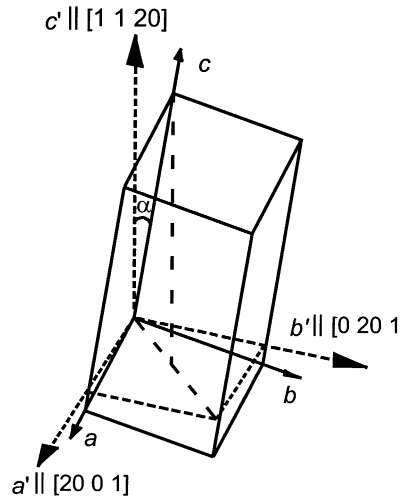

Fig. 1. Schematic of the (1 1 20)YBCO film growth on (7 10 2) $NdGaO_3$ substrates. The angles between crystallographic axes a, b, c of (1 1 20)YBCO film and a', b', c' of the "standard" (001)-oriented one on (110) $NdGaO_3$ substrate are $aa' = 7.6°$, $bb' = 7.9°$, $\alpha \equiv cc' = 11°$ correspondingly.

The surface structure of YBCO films was investigated by Atomic Force Microscope (AFM). Fig. 2(a) presents the result of the cross-section analysis of the typical c-axis oriented YBCO film. One can see that the maximum peak-to-valley roughness of the film surface is 3–4 nm, corresponding to the tunneling area in the a–b-plane of YBCO less than 3% of the total one. This fact points out the dominant c-axis and negligible a–b-plane current transport in c-HJ fabricated in these films [7]. Maximum peak-to-valley roughness of the tilted film surface is much higher $(\approx 25$ nm$)$ and, in general, depends on the tilt angle (see Fig. 2(b).

After cooling down to 100°C and before vacuum breaking the YBCO films were *in-situ* coated with a 10 nm laser deposited Au overlay. Later on, 7–30 and 100 nm thick Au and

Manuscript received August 6, 2002. This work was supported in part by the INTAS projects N2001-0809 and N2001-0249, Swedish Foundation for Strategic Research within the OXIDE program, Russian Foundation for Basic Research N02-02-106724-ìàñ and N00-02-17046, and NATO Science for Peace program N973559.

G. A. Ovsyannikov, P. V. Komissinski, and Y. V. Kislinski are with the Institute of Radio Engineering and Electronics RAS, Moscow 101999, Russia (e-mail: gena@hitech.cplire.ru; filipp@hitech.cplire.ru; yuli@hitech.cplire.ru).

E. Il'ichev is with the Institute for Physical High Technology, Jena, D-07702, Germany (e-mail: ilichev@adam.ipht-jena.de).

Z. G. Ivanov is with Chalmers University of Technology and Gothenburg University, Gothenburg, S-41296, Sweden (e-mail: f4azi@fy.chalmers.se).

Digital Object Identifier 10.1109/TASC.2003.814077

[1]The suppression of the twin formation has been also observed for (1 1 20) YBCO films [6].

TABLE I
PARAMETERS OF THE MEASURED HETEROJUNCTIONS

	№	A μm^2	J_c A/cm^2	$R_N A$ $\mu\Omega \times cm^2$	$I_c R_N$ μV
c-HJ	SQ1J1	100	5	4.4	22
	SQ1J3	10000	1.81	15	27
	SQ1J5	100	1.5	18.3	27.5
	SQ3J1	100	1	68	68
	SQ7J10	225	6.7	11.5	76.5
	SQ7J11	10000	2.34	5	11.7
	SQ7J3	625	3.2	8.1	26
	SQ7J4	900	2.6	7.5	19.1
	SQ7J13	400	2.5	4	10
	SQ7J15	400	4	7.2	28.8
	SQ7J17	100	2	18.8	37.6
	SQ7J18	100	3	10	30
	SQ10J3	100	1.2	60	72
t-HJ	J9	100	45	6	270
	J10	400	2.5	60	150
	J11	900	1.4	108	156
	J12	900	0.2	360	80

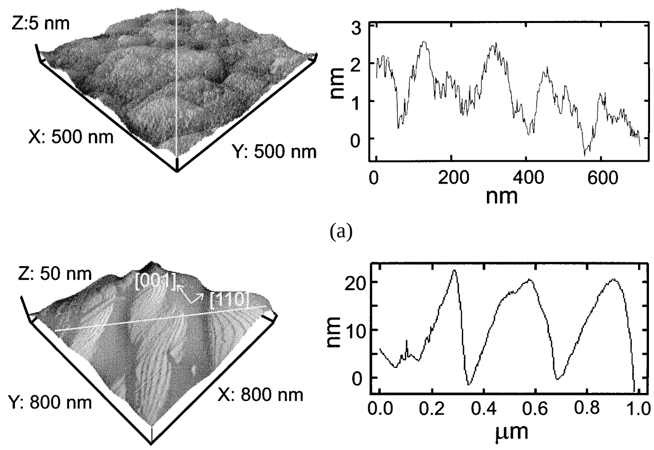

Fig. 2. AFM images of (a) c-axis and (b) (1 1 20)-oriented YBCO film surfaces (left parts) and the cross-sections (right parts) performed along the white lines on the corresponding left parts. The film thickness is 150 nm in both cases.

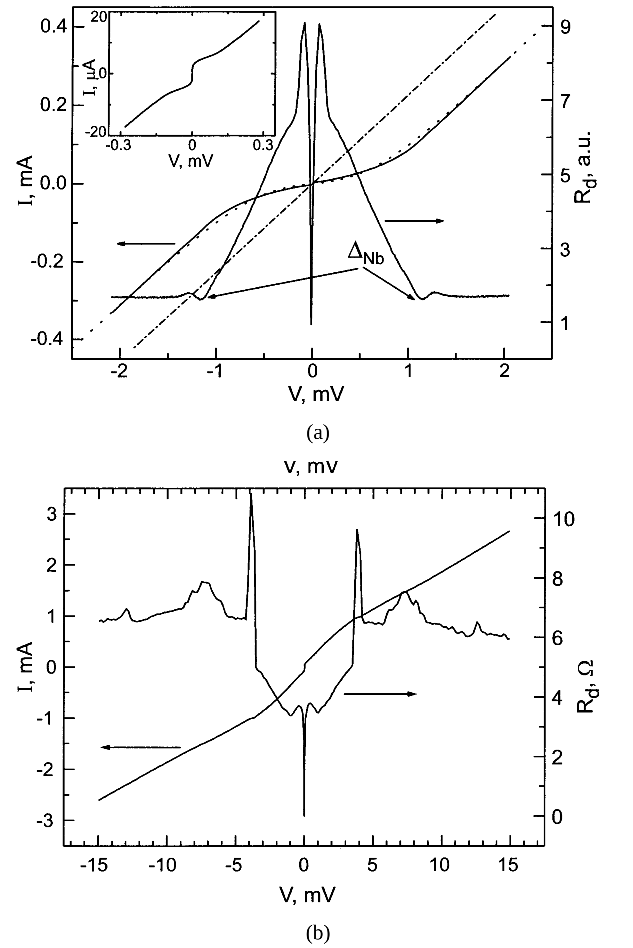

Fig. 3. (a) Typical I–V and $R_d(V)$ curves of the Nb/Au/YBCO c-HJ with a 20 nm thick Au film, measured at $T = 4.2$ K (solid lines). The fitting of the I–V curve to the (1) (dotted line) and the Ohm's law $V = IR_N$ (dash–dot line) are also shown. The inset presents the I–V curve at small voltages, $V \leq 300\ \mu$V; (b) I–V and $R_d(V)$ curves of the Nb/Au/YBCO t-HJ at $T = 4.2$ K.

Nb films were deposited using *ex-situ* electron beam evaporation and RF magnetron sputtering correspondingly. Photolitography and Ar ion milling techniques were used to pattern Nb/Au/YBCO multilayer into planar HJ of the areas $A = 5 \times 5$ to $100 \times 100\ \mu m^2$ [7].

Formation of undesirable edge contacts was prevented by evaporation and patterning of 200 nm thick insulating SiO_2 layer. 200 nm thick Au leads and contact pads allowed to perform 4-point electric measurements at temperatures 1.6 K $< T <$ 300 K and under influence of mm-wave radiation of 40–100 GHz. The table presents parameters of the measured HJ.

III. RESULTS AND DISCUSSION

A. I–V Curves

1) c-HJ: The I–V curves and differential resistance *vs*. bias voltage $R_d(V)$ dependences are shown in Fig. 3(a). The values of J_c for the c-HJ are $J_c = 1$–7 A/cm^2 at $T = 4.2$ K, whereas $I_c R_N = 10$–76 μV, where $R_N = R_d$ (2 mV) is the junction resistanse in the normal state. At $V < 1$ mV the I–V curves correspond to a Resistive Shunted Junction model (RSJ) of the Josephson junction with the small capacitance (see inset to the Fig. 3(a)). At high voltages the I–V curves of the c-HJ (Fig. 3(a)) can be approximated by the equation [8]

$$V = IR_N + I_e R_N \mathrm{th}\,(\mathrm{eV/KT}). \tag{1}$$

Usually, the excess current $I_e > 0$ can be observed in superconducting junctions with direct (nontunnel) conductivity. Current deficiency ($I_e < 0$) is a characteristic feature of the superconducting double-barier $S'/N/S$ HJ and exists together with the proximity effect in the N [8].

From the I–V curve of the junction shown in Fig. 3(a) one can determine $I_e = -145\ \mu$A at $T = 4.2$ K. Adopting the calculations [8] for this junction $I_e = (-\bar{D}\Delta_{\mathrm{YBCO}} - \Delta_{\mathrm{Nb}})/(eR_N) \approx -270\ \mu$A, where $\bar{D}$ is the transparency of the Au/YBCO interface averaged over the quasiparticle momentums. $\bar{D} = 2\rho_c l/(3r) = 10^{-4}$–$10^{-5}$ is determined by $r = R_N A = 10^{-5}$–$10^{-6}\ \Omega \cdot \mathrm{cm}^2$. Here $\rho_c \approx 10^{-2}\ \Omega \cdot$ cm and $l \approx 1$ nm is the resistivity and mean free path in c-axis direction of YBCO film, $\Delta_{\mathrm{YBCO}} \approx 20$ mV

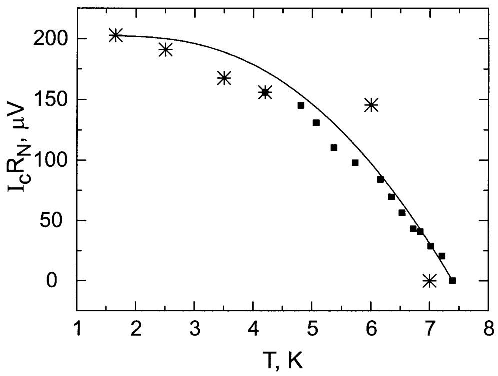

Fig. 4. The experimental $I_c(T)R_N$ dependences for the c-HJ (stars) and t-HJ (squares). Solid line: $I_c(T)R_N$ calculated from the (2) using $T_{c\mathrm{Nb}} = 7.4$ K, $\Delta_d = 20$ mV, $\Delta_s(0) = \Delta_{\mathrm{Nb}}(0) = 1.2$ mV and BCS temperature dependence of $\Delta_{\mathrm{Nb}}(T)$. The experimental points for c-HJ are normalized by a factor of $\delta \approx 0.48$ to fit the (2) at $T = 1.7$ K: if the finite s-wave component is admixed to the d-wave YBCO order parameter and it does change sign across the twin boundary [3] the net first order I_c in c-HJ is reduced compare to the quasiclassical model [7], [11].

and $\Delta_{\mathrm{Nb}} = 1.2$ mV are YBCO and Nb superconducting gaps correspondingly [2].

The observed dip in $R_d(V)$ at $V = 1.2$ mV and its temperature dependence corresponds to Δ_{Nb} (Fig. 3(a)) and disappears together with the critical current at $T = 8.5$–9.1 K. Note that similar gap features associated with s-wave superconductor (Pb) were previously observed in c-HJ Pb/YBCO [1].

2) t-HJ: Fig. 3(b) shows the I–V curve and $R_d(V)$ dependence for one of the t-HJ at $T = 4.2$ K. The narrow minimum around zero voltage and dip of the $R_d(V)$ at $V = 1.2$ mV characterize the critical current and Δ_{Nb} correspondingly (Fig. 3(b)). For the t-HJ the critical current density is of the same order of magnitude as for the c-HJ: $j_c = 1 - 45$ A/cm^2 at $T = 4.2$ K, while the values of $I_cR_N = 80$–270 μV are higher. But the I–V curves for the t-HJ differ significantly from ones for the c-HJ. The relatively broad minimum of $R_d(V)$ at $V < 5$ mV (caused by zero energy midgap states (MGS) near the surface of d-wave superconductor) can be clearly observed in the I–V curves of the t-HJ (Fig. 3(b)) [9]. The excess current $(I_e \approx I_c)$ is also presented in these I–V curves. So, the current transport through MGS is quite significant [9].

B. Critical Current

1) c-HJ: Fig. 4 presents the experimentally obtained $I_cR_N(T)$ dependences for the c-HJ (stars) and t-HJ (squares). Since no minimum of $R_d(V)$ associated with the MGS has been observed for the c-HJ, we can fit their experimental $I_cR_N(T)$ dependence within the quasiclassical model of the superconducting current flowing through the energy states near the superconducting gap [7], [10], [11][2]

$$I_cR_N = \frac{\Delta_s \Delta_{\mathrm{Nb}} 2\ln\left(\frac{3.6\Delta_d}{kT_{c\mathrm{Nb}}}\right)}{(\pi e \Delta_d)}, \tag{2}$$

[2]The resistance of the Au/YBCO interface is about 10^3 times higher than that of the Nb/Au one, so we can neglect the contribution of the latter to the total resistance.

assuming that $\Delta_{\mathrm{YBCO}} = \Delta_s + \Delta_d \cos 2\theta$, where the angle θ determines the direction of the quasiparticles momentum, Δ_d and Δ_s are the d- and s-wave superconducting gaps of YBCO correspondingly, $\Delta_d \gg \Delta_s, \Delta_{\mathrm{Nb}}$, and k is the Boltzmann constant.

The result of the calculations using the (2) is shown in Fig. 4 (solid line) for $T_{c\mathrm{Nb}} = 7.4$ K, $\Delta_d = 20$ mV, $\Delta_s(0) = \Delta_{\mathrm{Nb}}(0) = 1.2$ mV and BCS temperature dependence of $\Delta_{\mathrm{Nb}}(T)$.

2) t-HJ: There are zero energy MGS levels in t-HJ on (110)-oriented d-wave superconductor $(S/D_{(110)})$ [9], [12]

$$E_n(\varphi) = \pm \frac{\Delta_l \Delta_d D(\theta) \sin\varphi}{[2\Delta_l + D(\theta)(\Delta_d - \Delta_l)]}, \tag{3}$$

where Δ_1 is the superconducting gap of the s-wave superconductor (Δ_{Nb}). These MGS levels are, in fact, the additional channels for superconducting current. At low temperatures (case (i)) $(kT \ll \bar{D}\Delta_d)$ a significant contribution of MGS-channels to $I_c \propto \bar{D}$ and the low-temperature peak in $I_c(T)$ together with the nonsinusoidal CPR $I_s(\varphi) \propto \mathrm{sign}(\sin\varphi)\cos\varphi$ $(0 < \varphi < \pi)$ can be observed [12]. At higher temperatures (case (ii)) $(\bar{D}\Delta_d \le kT) I_c \propto \bar{D}^2$, $I_cR_N \sim \Delta_d^2 D/ekT$, and $I_s(\varphi) \propto \sin 2\varphi$.

In the experimentally studied t-HJ Nb/Au/YBCO at $T = 4.2$ K$\bar{D} \sim 10^{-4}$–10^{-5}, and, assuming $\Delta_d = 20$ m eV, $\bar{D}\Delta_d/k \sim 0.01$ K < 4.2 K, i.e., the case (ii) is realized. Taking $\bar{D} \sim 10^{-4}$ we have $I_cR_N < 2$ μV which is very small value compare to the experimentally measured $I_cR_N > 100$ μV. In addition, the experimental $I_c(T)$ decreases with the increase of temperature and has no low temperature peak. Therefore, we can neglect the zero energy MGS channel of the superconducting current in our t-HJ Nb/Au/YBCO and use the (2) to fit the experimental $I_cR_N(T)$ dependence.

IV. Current-Phase Relation

CPR measurements were performed using two different techniques: a single-junction interferometer configuration (RF-SQUID) [13] and measurements of the amplitudes of the critical current and Shapiro steps arising on the I–V-curves of the junction under external monochromatic electromagnetic radiation of frequency f_e[14]. Within the RSJ model for $\omega = 2\pi h f_e/2eI_cR_N \ge 1$ the amplitudes of the CPR harmonics determine the maximum values of the sub-harmonic Shapiro steps. The sub-harmonic Shapiro step on the I–V curve indicates the deviation of the CPR from the sinusoidal shape [15].

1) c-HJ: The typical CPR dependence of the c-HJ, obtained from the RF-SQUID measurements is shown in Fig. 5. At $T = 6$ K it has the sinusoidal shape. However, with decrease of temperature the deviation of CPR from $\sin\varphi$ develops. At $T = 4.2$ K the ratio between the first and second harmonics of the CPR is $I_1/I_2 \approx 0.12$. The maximum $I_1/I_2 \approx 0.16$ has been observed at the lowest measured temperature of $T = 1.7$ K.

Measuring another c-HJ on the same chip with the high-frequency technique at $f_e = 40$ GHz the first harmonic and sub-harmonic Shapiro steps with $I_{1/2}/I_1 \approx 0.08$ have been observed at $T = 4.2$ K.

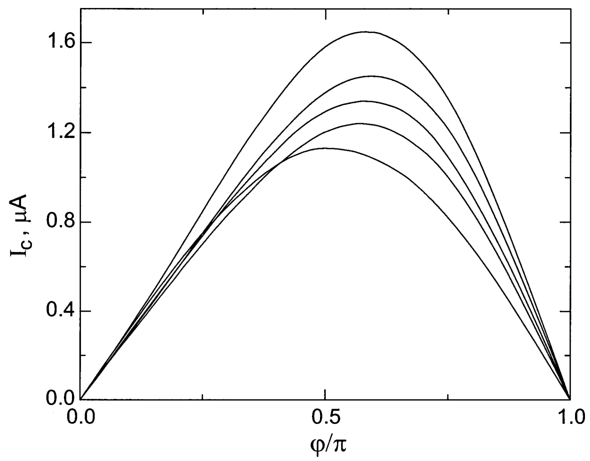

Fig. 5. The experimental current-phase relation of the Nb/Au/YBCO c-HJ J9 at $T = 1.7$, 2.5, 3.5, 4.2, and 6.0 K (from top to bottom) measured by the RF-SQUID technique.

Thus, the deviation of the CPR from the sinusoidal shape for c-HJ has been experimentally observed using both techniques and caused by the dominant d-wave order parameter symmetry in YBCO.

2) t-HJ: To estimate the CPR of the t-HJ we have measured I–V curves under monochromatic radiation of $f_e = 40$–100 GHz. The first harmonic Shapiro step observed in the I–V curve is symmetrical around the autonomous one at small amplitudes of the external radiation pointing the coherence of the Josephson oscillations in the studied t-HJ. However, no sub-harmonic Shapiro steps have been observed in the I–V curves within the measurement accuracy, which is determined by the noise current I_f. The latter is equal to the maximum deviation (in current) of the I–V curve from the autonomous one at $R_d \approx R_N/2$ near the Shapiro step [16] and for our measurement system is $I_f = 0.4$ μA at $T = 4.2$ K, so any steps larger than the I_f can be experimentally detected.

The observed maximum of the first Shapiro step is 11 μA for the measured t-HJ and, again, no sub-harmonic Shapiro steps have been observed. Thus, the CPR of this t-HJ is $I_s(\varphi) \propto \sin\varphi$ with the accuracy of 9% from the autonomous I_c value.

The absence of the second harmonic of the CPR in t-HJ Nb/Au/YBCO following from the d-wave symmetry of the superconducting order parameter in YBCO probably is caused by the small transparency of the Au/YBCO interface $\bar{D} \sim 10^{-4}$–10^{-5}. Note, that in the asymmetrical 45° bicrystal Josephson junctions the averaged transparency $\bar{D} \sim 10^{-2}$ can be realized and the CPR is strongly nonsinusoidal [17].

In conclusion, Nb/Au/YBCO HJ fabricated in c-axis oriented and tilted YBCO thin films showed superconducting current flowing through the energy states near the superconducting gap. The measurements of the superconducting current-phase relation of these junctions using RF-SQUID and microwave techniques revealed strong deviation of the CPR from the $\sin\varphi$ behavior for c-HJ, following from the d-wave symmetry of the superconducting order parameter in YBCO. The measured CPR of the t-HJ is of the sinusoidal shape with the accuracy of 9% from the autonomous I_c value.

Acknowledgment

The authors would like to thank M. Grajcar, R. Hlubina, I. V. Borisenko, K. I. Constantinian, and P. B. Mozhaev for their help in the experiments and fruitful discussions.

References

[1] C. C. Tsuei and J. K. Kirtley, *Rev. Mod. Phys.*, vol. 72, no. 4, pp. 969–1016, Oct. 2000.
[2] J. W. T. Wei, N.-C. Yeh, D. F. Garrigus, and M. Strasik, *Phys. Rev. Lett.*, vol. 81, no. 12, pp. 2542–2545, Sept. 1998.
[3] K. A. Kouznetsov *et al.*, *Phys. Rev. Lett.*, vol. 79, no. 16, pp. 3050–3053, Oct. 1997.
[4] Y. Tanaka, *Phys. Rev. Lett.*, vol. 72, no. 24, pp. 3871–3874, June 1994.
[5] M. Y. Kupriyanov and K. K. Likharev, *IEEE Trans. Magn.*, vol. 27, no. 2, pp. 2460–2463, March 1991.
[6] I. K. Bdikin, P. B. Mozhaev, G. A. Ovsyannikov, F. V. Komissinskii, I. M. Kotelyanskii, and E. I. Raksha, *Physics of the Solid State*, vol. 43, no. 9, pp. 1611–1620, 2001.
[7] P. V. Komissinski *et al.*, *Europhys. Lett.*, vol. 57, no. 4, pp. 585–591, Febr. 2002.
[8] A. F. Volkov, A. V. Zaitsev, and T. M. Klapwijk, *Physica C*, vol. 210, pp. 21–34, 1993.
[9] T. Löfwander, V. S. Shumeiko, and G. Wendin, *Supercond. Sci. Technol.*, vol. 14, pp. R53–77, 2001.
[10] A. V. Zaitsev, *Sov. Phys. JETP*, vol. 59, p. 1015, 1984.
[11] A. Furusaki and M. Tsukada, *Phys. Rev. B*, vol. 43, no. 13, pp. 10 164–10 169, May 1991.
[12] R. A. Riedel and P. F. Bagwell, *Phys. Rev. B*, vol. 57, no. 10, pp. 6084–6089, March 1998.
[13] E. Il'ichev *et al.*, *Rev. Sci. Instr.*, vol. 72, no. 3, pp. 1882–1887, March 2001.
[14] V. N. Gubankov, V. P. Koshelets, and G. A. Ovsyannikov, *Sov. Phys. JETP*, vol. 44, p. 181, 1976.
[15] R. Kleiner *et al.*, *Phys. Rev. Lett.*, vol. 76, no. 12, pp. 2161–2164, March 1996.
[16] K. K. Likharev, *Rev. Mod. Phys.*, vol. 51, p. 101, 1979.
[17] E. Il'ichev *et al.*, *Phys. Rev. B*, vol. 60, no. 5, pp. 3096–3099, August 1999.